Inorganic Chemistry

Article

pubs.acs.org/IC

# Synthesis, Crystal Structure, and Magnetic Characterization of the Three-Dimensional Compound $[Co_2(cbut)(H_2O)_3]_n$ ($H_4cbut$ = 1,2,3,4-Cyclobutanetetracarboxylic Acid)

Pau Díaz-Gallifa,[†] Oscar Fabelo,*[,‡,§] Jorge Pasán,*[,†] Laura Cañadillas-Delgado,[∥] Juan Rodríguez-Carvajal,[‡] Francesc Lloret,[⊥] Miguel Julve,[⊥] and Catalina Ruiz-Pérez[†]

[†]Laboratorio de Rayos X y Materiales Moleculares, Departamento de Física, Universidad de La Laguna, Tenerife, Avda. Astrofísico Francisco Sánchez s/n, E-38204, La Laguna, Tenerife Spain

[‡]Institut Laue-Langevin, Grenoble, 71 avenue des Martyrs, C.S. 20156, 38042 Grenoble Cedex 9, France

[§]Instituto de Ciencia de Materiales de Aragón, CSIC-Universidad de Zaragoza, C/Pedro Cerbuna 12, E-50009, Zaragoza, Spain

[∥]Centro Universitario de la Defensa de Zaragoza, Ctra de Huesca s/n, 50090 Zaragoza, Spain

[⊥]Instituto de Ciencia Molecular/Departament de Química Inorgànica, Universitat de València, C/Catedrático José Beltrán 2, 46980 Paterna, València, Spain

Supporting Information

**ABSTRACT:** A novel cobalt(II) complex of formula $[Co_2(cbut)(H_2O)_3]_n$ (**1**) ($H_4cbut$ = 1,2,3,4-cyclobutanetetracarboxylic acid) has been synthesized under hydrothermal conditions and its crystal structure has been determined by means of synchrotron radiation and neutron powder diffraction. The crystal structure of **1** consists of layers of cobalt(II) ions extending in the *bc*-plane which are pillared along the crystallographic *a*-axis through the skeleton of the $cbut^{4-}$ ligand. Three crystallographically independent cobalt(II) ions [Co(1), Co(2), and Co(3)] occur in **1**. They are all six-coordinate with four carboxylate-oxygens [Co(1)−Co(3)] and two *cis*-[Co(1)] or *trans*-water molecules [Co(2) and Co(3)] building distorted octahedral surroundings. Regular alternating double oxo(carboxylate) [between Co(1) and Co(1a)] and oxo(carboxylate) plus one aqua and a *syn*−*syn* carboxylate bridges [between Co(1) and Co(2)] occur along the crystallographic *b*-axis, the values of the cobalt−cobalt separation being 3.1259(8) and 3.1555(6) Å, respectively. These chains are connected to the Co(3) atoms through the OCO carboxylate along the $[0\bar{1}1]$ direction leading to the organic−inorganic *bc*-layers with Co(1)−$OCO_{(anti-syn)}$−Co(3) and Co(2)−$OCO_{(anti-anti)}$−Co(3) distances of 5.750(2) and 4.872(1) Å. The shortest interlayer cobalt−cobalt separation through the $cbut^{4-}$ skeleton along the crystallographic *a*-axis is 7.028(2) Å. Variable-temperature magnetic susceptibility measurements show the occurrence of antiferromagnetic ordering with a Néel temperature of 5.0 K, followed by a field-induced ferromagnetic transition under applied dc fields larger than 1500 Oe. The magnetic structure of **1** has been elucidated at low temperatures in zero field by neutron powder diffraction measurements and was found to be formed by ferromagnetic chains running along the *b*-axis which are antiferromagnetically coupled with the Co(3) ions through the *c*-axis giving rise to noncompensated magnetic moments within each *bc*-layer (ferrimagnetic plane). The occurrence of an antitranslation operation between these layers produces a weak interlayer antiferromagnetic coupling along the *a*-axis which is overcome by dc fields greater than 1500 Oe resulting in a phase transition toward a ferromagnetic state (metamagnetic behavior).

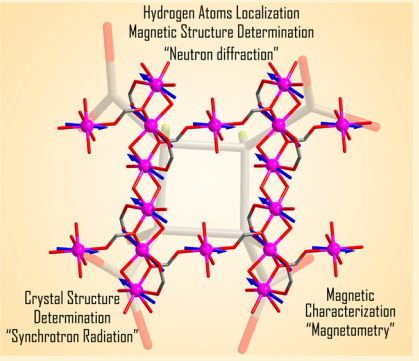


## INTRODUCTION

Molecule-based magnets arising from the assembling of discrete chemical objects (mono- or polynuclear entities, metal ions, and ligands) have being extensively explored in the past decade because of their potential application in electronic and magnetic devices, electromagnetic shielding and information storage.[1] These new materials have some advantages over the conventional ones such as their optical transparency, flexibility, biocompatibility, structural diversification, and the low production costs because most of them are obtained at relatively low temperatures. However, the control of the crystal packing to produce well-defined architectures is a key point and it remains a challenge.[2] This is due to the variety of parameters involved in the building strategy: the coordination geometry of the metal ions, the flexibility of the ligand backbones, the metal/ligand molar ratios, the presence of counterions and solvents, the binding properties of the ligand, the chemical affinity between the different component and proper or improper symmetry relations, among others. Even using the

**Received:** February 25, 2014

   dx.doi.org/10.1021/ic500443t | *Inorg. Chem.* XXXX, XXX, XXX−XXX

same reactants with the same metal/ligand ratios, subtle changes in the synthesis conditions may lead to different frameworks and topologies.[3] This is why systematic studies of the different crystallization conditions are required to get a reasonable "knowledge" of the variable parameters that allow the rational design of new functional frameworks.

Among the diversity of metal ions and connectors involved in the synthesis of magnetic metal organic frameworks (MOFs), the cobalt(II) ion and polycarboxylate ligands are very appealing.[4] At one hand, the high-spin six-coordinate Co(II) ion ($3d^7$ configuration) has a $^4T_{1g}$ ground state in $O_h$-symmetry where the angular momentum is not fully quenched and contributes to a large magnetic anisotropy through the spin−orbit coupling;[5] although the degeneracy of this $^4T_{1g}$ electronic ground state is partially lifted into the $^4A_{2g}$ and $^4E_g$ levels under an axial distortion ($D_{4h}$ point group), when such a distortion ($\Delta$) is similar in magnitude to the spin−orbit coupling ($\lambda$), both perturbations have to be taken into consideration. These features make the Co(II) ion in a slightly distorted octahedral geometry a suitable candidate to build anisotropic magnetic systems, such as single-ion magnets (SIMs),[6] single-molecule magnets (SMMs),[7] or single-chain magnets (SCMs).[8] On the other hand, the carboxylate group is a highly versatile ligand because in addition to its monodentate and chelating coordination modes, it can adopt *syn*−*syn*, *anti*−*syn*, and *anti*−*anti* conformations when acting as a bridge between metal ions; being able to mediate ferro- or antiferromagnetic interactions in this last case, as illustrated by the extensive literature on the carboxylate-bridged copper(II) complexes.[9]

As far as the carboxylate-bridged high-spin cobalt(II) ions are concerned, the number of magnetostructural studies is much more reduced becaue of the complicated analysis of their magnetic properties arising from the spin−orbit coupling effects. Anyway, weak antiferromagnetic interactions across the *syn*−*syn* conformation[10] and either ferro- or antiferromagnetic interactions through the *anti*−*anti*[11] and *anti*−*syn*[12] conformations were reported. In an attempt to extend these magnetic anisotropic systems to high-dimensional networks thinking at their potential application as multifunctional materials, more or less rigid aromatic polycarboxylate ligands, such as phenylenediacetate ($phda^{2-}$),[13] 1,4-benzenedicarboxylate ($bda^{2-}$),[14] 1,2,4-benzenetricarboxylate ($btc^{3-}$),[15] or 1,2,4,5-benzenetetracarboxylate ($bta^{4-}$),[13b,15c,16] have been used. The determination of the orientation of the magnetic moments of the interacting cobalt(II) ions in these high-dimensional systems is of particular interest to understand their complicated magnetic behaviors. Neutron diffraction is the most direct method to determine bulk magnetic structure.[17] The Co(II) hydroxide terephtalate compound presented by Drillon et al.[14a] or our recent Co(II) pyromellitate complex[16a] are illustrative examples of the application of this nonextended technique into inorganic−organic compounds.[18]

In this Article, we report the synthesis and magnetostructural study of a new three-dimensional polycarboxylate-cobalt(II) system of formula $[Co_2(cbut)(H_2O)_3]_n$ (**1**) ($H_4$cbut =1,2,3,4-cyclobutanetetracarboxylic acid), whose magnetic structure has been elucidated at lower temperatures in zero field by neutron powder diffraction measurements.

## EXPERIMENTAL SECTION

**Materials and Methods.** Reagents and solvents used in the syntheses were purchased from commercial sources and used without further purification. Elemental analyses (C, H, N) were performed with an EA 1108 CHNS/0 automatic analyzer. IR spectrum on a powder sample of **1** was performed on a IR Affinity-1 FTIR spectrophotometer in the 4000−400 $cm^{-1}$ range equipped with a Pike Technologies GladiATR. All of our attempts to grow single crystals of **1** in deuterated water were unsuccessful.

**Synthesis of $[Co_2(cbut)(H_2O)_3]_n$ (1).** Ammonia solution (25% v/v in water) was added dropwise to an aqueous solution (15 mL) of $H_4$cbut (0.5 mmol, 0.116 g) until a pH value of 4.5 was attained. Then, an aqueous solution (10 mL) of $Co(NO_3)_2{\cdot}6H_2O$ (0.291 g, 1 mmol) was slowly poured into that solution. The resulting mixture was sealed in a 45 mL stainless-steel reactor with a Teflon linear, and it was heated at 170 °C during 48 h. X-ray quality crystals of **1** as an aggregate of dark pink plates were obtained after cooling. It should be noted that an *in situ* reaction transformation from the commercial *trans*−*cis*−*trans*-1,2,3,4-cyclobutanetetracarboxylic acid toward the *trans*−*trans*−*trans*-1,2,3,4-cyclobutanetetracarboxylate ligand occurs during the hydrothermal process.[19] Yield (based on the cobalt): ca. 60%. Anal. Calcd for $C_8H_{10}Co_2O_{11}$ (**1**): C, 24.02; H, 2.52%. Found: C, 23.93; H, 2.55%. FT-IR: 3508 (w), 3080(w), 1558(s), 1417(s), 1278(m), 1244(m), 748(s), 640(s), 555(s).

**Physical Measurements.** Magnetic susceptibility measurements on a polycrystalline sample of compound **1** were carried out in the temperature range 2−300 K with a Quantum Design SQUID magnetometer under applied magnetic fields of 1000 Oe ($2 \leq T \leq 30$ K) and 5000 Oe ($30 < T \leq 300$ K). The magnetization measurements were performed at 2.0 K in the field range ±50 kOe. Diamagnetic corrections of the constituent atoms were estimated from Pascal's constants[20] being $-156 \times 10^{-6}$ $cm^3$ $mol^{-1}$ [per two Co(II) ions]. The experimental magnetic susceptibility data were also corrected for the magnetization of the sample holder (a plastic bag).

**X-ray Crystal Structure Determination and Refinement.** Single crystal X-ray diffraction data of a single crystal of **1** were collected at 100 K using synchrotron radiation (at the ESRF Spanish beamline BM16) with a $\lambda$ = 0.7383 Å and a CCD ADSCq210rCCD detector. A phi scan strategy was followed in the data collection with an oscillation range ($\Delta\varphi$) for each image of one degree. Two different orientations of the crystal were measured in order to increase the data completeness. Data were indexed, integrated and scaled using the HKL2000 program.[21] The structure was solved by direct methods and subsequent Fourier syntheses using the SHELXS-97,[22] and it was refined by the full-matrix least-squares technique against $F^2$ using with the SHELXL-97 program.[22] Anisotropic thermal parameters were used to refine all non-hydrogen atoms. The hydrogen atoms of the water molecules were not located by the X-ray diffraction data, however, those of the cbut ligand were set on geometrical position and refined with a riding model. The final geometrical calculations and the graphical manipulations were carried out with the PLATON[23] and DIAMOND[24] programs. A summary of the crystal data and refinement conditions is listed in Table 1, whereas selected bond lengths and angles are shown in Table 2. Crystallographic data for the structure of **1** has been deposited at the Cambridge Crystallographic Data Centre with CCDC reference number 983489.

**Neutron Powder Diffraction.** Neutron powder diffraction experiments were performed on the high-resolution multidetector D2B at ambient conditions and on the high-intensity diffractometer D20 in a variable temperature environment at


dx.doi.org/10.1021/ic500443t | Inorg. Chem. XXXX, XXX, XXX−XXX

**Table 1. Crystal Data and Details of the Structure Determination for Complex 1**

| | |
|---|---|
| formula | $C_8H_{10}Co_2O_{11}$ |
| fw | 400.02 |
| crystal system | Triclinic |
| space group | $P\bar{1}$ |
| $a$ (Å) | 7.5240(15) |
| $b$ (Å) | 9.3200(19) |
| $c$ (Å) | 9.7440(19) |
| $\alpha$ (deg) | 89.01(3) |
| $\beta$ (deg) | 71.16(3) |
| $\gamma$ (deg) | 74.82(3) |
| $V$ (Å$^3$) | 622.4(2) |
| $Z$ | 2 |
| $\mu$ (cm$^{-1}$) | 2.980 |
| $T$ (K) | 100 |
| $\rho_{calcd}$ (g cm$^{-3}$) | 2.134 |
| $\lambda$ (Å) | 0.738 30 |
| index ranges | $-9 \le h \le 9$ |
| | $-11 \le k \le 11$ |
| | $-11 \le l \le 12$ |
| total reflns | 10 085 |
| indep. reflns ($R_{int}$) | 2572 (0.0464) |
| obsd reflns [$I > 2\sigma(I)$] | 2533 |
| parameters | 194 |
| GOF | 0.926 |
| $R$ [$I > 2\sigma(I)$] | 0.0300 |
| $R_w$ [$I > 2\sigma(I)$] | 0.0854 |
| $R$ [all data] | 0.0304 |
| $R_w$ [all data] | 0.0871 |

the Institut Laue Langevin (Grenoble, France). The sample was contained in a ⌀6 mm cylindrical vanadium can and, in the case of D20, this sample container was placed inside a vanadium-tailed Orange Cryostat (69ILHV25). The diffraction patterns were recorded using the wavelengths $\lambda$ = 1.5946 (at D2B) and 2.4095 Å (at D20). The structures were refined by the Rietveld method using the FullProf program.[25]

**Neutron Nuclear Structure Refinement.** A data set was collected on the high-resolution neutron diffractometer, D2B, with the aim of determining precisely the hydrogen positions for **1**. The initial model obtained from the previous synchrotron single crystal X-ray diffraction experiment was been used as starting point for the Rietveld refinement (see Figure 1). The determination and refinement of the cell parameters as well as the non-hydrogen atoms at 300 K was carried out without any restriction. The position and the isotropic atomic displacement parameter of the hydrogen atoms from coordination water molecules were refined using restrains (soft constraints) (see Figure 2). The atomic positions obtained from the high resolution neutron diffraction refinements compared with those obtained from single crystal X-ray diffraction are shown in Supporting Information Table S1.

The temperature dependence of the neutron diffraction patterns of **1** collected from 2 to 14 K at the D20 diffractometer shows that the nuclear structure remains unchanged in the whole observed temperature range (see Supporting Information Figure S1); nevertheless, low angle magnetic reflections start to increase at ∼5 K corresponding to the Néel transition temperature (see Figure 3). This increase of the intensity is compatible with the occurrence of long-range antiferromagnetic ordering.

## RESULTS AND DISCUSSION

**Description of the Structure of 1.** Complex **1** has a three-dimensional structure which is made up by organic−inorganic layers of cobalt(II) ions extended into the *bc*-plane that are pillared along the crystallographic *a*-axis through the skeleton of the cbut$^{4-}$ ligand, exhibiting a regular *AAA* sequence (Figure 4). Each layer is formed by ···Co(2)Co(1)Co(1)$^{(a)}$Co(2)$^{(f)}$··· edge sharing chains which run along the crystallographic *b*-axis [see Figure 5(top)]. Two different bridges connect the Co(II) ions within this chain. The Co(1) and Co(1)$^{(a)}$ atoms are linked by a double $\mu$-oxo(carboxylate) [O(6) and O(6)$^{(a)}$] with a separation between the metal atoms of 3.1259(8) Å and an angle at the bridgehead O(6) atom of 96.83(2)°. However,

**Table 2. Selected Bond Lenghs (Å) and Angles (deg) for 1[a]**

| | | | |
|---|---|---|---|
| Co(1)−O(2) | 2.076(2) | Co(2)−O(2) | 2.152(2) |
| Co(1)−O(6) | 2.088(2) | Co(2)−O(7)$^b$ | 1.990(2) |
| Co(1)−O(6)$^a$ | 2.089(2) | Co(2)−O(9w) | 2.144(2) |
| Co(1)−O(8)$^b$ | 2.104(2) | Co(3)−O(1) | 2.032(2) |
| Co(1)−O(9w) | 2.107(2) | Co(3)−O(4) | 2.142(2) |
| Co(1)−O(10w) | 2.062(2) | Co(3)−O(11w) | 2.136(2) |
| O(2)−Co(1)−O(6) | 105.26(6) | O(6)$^a$−Co(1)−O(8)$^b$ | 84.47(7) |
| O(2)−Co(1)−O(10w) | 96.82(8) | O(2)−Co(2)−O(7)$^b$ | 88.89(7) |
| O(2)−Co(1)−O(9w) | 81.35(6) | O(2)−Co(2)−O(7)$^a$ | 91.11(7) |
| O(2)−Co(1)−O(6)$^a$ | 169.02(6) | O(2)−Co(2)−O(9w) | 78.79(6) |
| O(2)−Co(1)−O(8)$^b$ | 88.48(7) | O(2)−Co(2)−O(9w)$^c$ | 101.21(6) |
| O(6)−Co(1)−O(6)$^a$ | 83.10(6) | O(9w)−Co(2)−O(7)$^d$ | 88.01(7) |
| O(6)−Co(1)−O(8)$^b$ | 89.24(7) | O(9w)−Co(2)−O(7)$^c$ | 91.99(7) |
| O(6)−Co(1)−O(9w) | 173.21(6) | O(1)−Co(3)−O(4) | 97.14(7) |
| O(6)−Co(1)−O(10w) | 85.78(7) | O(1)−Co(3)−O(4)$^e$ | 82.86(7) |
| O(9w)−Co(1)−O(10w) | 91.93(7) | O(1)−Co(3)−O(11w) | 87.61(8) |
| O(9w)−Co(1)−O(6)$^a$ | 90.54(6) | O(1)−Co(3)−O(11w)$^e$ | 92.39(9) |
| O(9w)−Co(1)−O(8)$^b$ | 92.55(7) | O(4)−Co(3)−O(11w) | 92.70(7) |
| O(10w)−Co(1)−O(6)$^a$ | 90.82(7) | O(4)−Co(3)−O(11w)$^e$ | 87.30(8) |
| O(10w)−Co(1)−O(8)$^b$ | 173.52(6) | | |

[a]Symmetry codes: (a) $-x + 1, -y, -z + 1$; (b) $x + 1, y, z$; (c) $-x + 1, -y + 1, -z + 1$; (d) $-x, -y + 1, -z + 1$; (e) $-x + 1, -y + 1, -z$.


dx.doi.org/10.1021/ic500443t | Inorg. Chem. XXXX, XXX, XXX−XXX

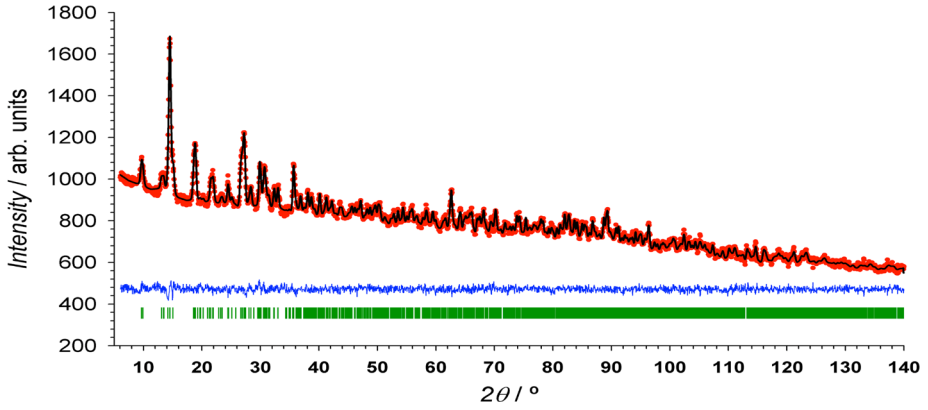


**Figure 1.** Neutron diffraction pattern of **1** at 300 K using a D2B diffractometer with $\lambda$= 1.5946 Å. The refinement has been done in the space group $P\bar{1}$ with the associated cell parameters $a$ = 7.51934(20) Å, $b$ = 9.3120(3) Å, $c$ = 9.7415(3) Å, $\alpha$ = 88.980(3)°, $\beta$ = 71.158(2)°, and $\gamma$ = 74.793(2)°, with the following statistics $\chi^2$ = 1.43 and $R_B$ = 5.33%. The experimental and calculated data are represented as red circles and a black solid line respectively, whereas the blue line is the difference between them and the green vertical lines correspond to the Bragg positions.

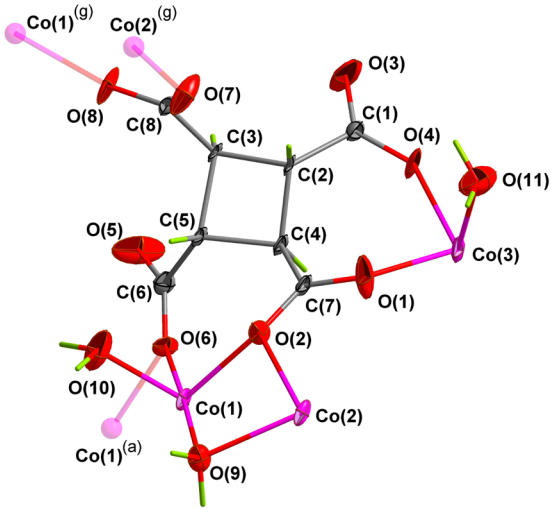


**Figure 2.** View of a fragment of the structure of **1** together with the atom numbering, obtained from the high-resolution neutron refinement at 300 K. The ORTEP mode has been used to denote the asymmetric unit. For the sake of clarity, transparent and stick modes were used to represent the atoms generated by symmetry operations and the hydrogen atoms, respectively. Symmetry code: (a) $-x + 1$, $-y$, $-z + 1$; (g) $x - 1$, $y$, $z$.

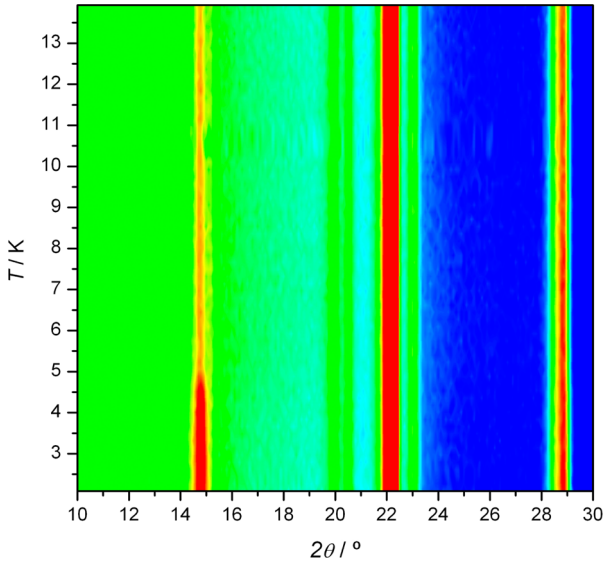


**Figure 3.** Mesh plot of **1** collected at the neutron powder diffractometer D20 in the temperature range 2−14 K, showing the increase of intensity at $T_c$ (~5 K) because of the occurrence of magnetic ordering.

Co(1) and Co(2) are bridged by one water molecule [O(9w)], a $\mu$-oxo(carboxylate) [O(2)] and a carboxylate group in the *syn*−*syn* conformation [O(8)$^{(b)}$−C(8)$^{(b)}$−O(7)$^{(b)}$] with a separation of 3.1555(6) Å [Co(1)$^{\cdots}$Co(2)] and the bridgehead angles Co(1)−O(9w)−Co(2) and Co(1)−O(2)−Co(2) of 96.11(2)° and 96.57(2)°, respectively. These chains are connected to the Co(3) atoms through the carboxylate O(1)−C(7)−O(2) groups along the [0$\bar{1}$1] direction, the metal center acting as a node between two adjacent chains and leading to the organic−inorganic *bc*-layers [Co(1)−OCO−Co(3) and Co(2)−OCO−Co(3) distances of 5.750(2) and 4.872(1) Å] [see Figure 5 (bottom)]. It deserves to be noted that three of the four carboxylate groups of each cbut$^{4-}$ ligand are involved in the building of the organic−inorganic layer while the remaining carboxylate group [O(7)−C(8)−O(8)] is coordinated to the adjacent layer. Therefore, the whole ligand act as connector along the *a*-axis between different layers, forming the final three-dimensional structure observed in **1**. The shortest interlayer cobalt−cobalt separation along the crystallographic *a*-axis is 7.524(2) Å. From a topological point of view, this complex exhibits - ($4^4{\cdot}6^2$) and 5-fold ($4^4{\cdot}6^6$) nodes that give rise to a *fsc-4,5-**Cmmm*** (in Schläfli notation) topological network [see Figure 4 (right)].[26]

Three crystallographically independent cobalt(II) ions [Co(1), Co(2), and Co(3)] are present in **1**, two of them, Co(2) and Co(3) laying on inversion centers (see Figure 2). They are all six-coordinate with two coordinated water molecules in *cis*- [Co(1)] or *trans*-positions [Co(2) and Co(3)] and four carboxylate-oxygen atoms from different cbut$^{4-}$ ligands describing somewhat compressed octahedra. The O(2), O(6)$^{(a)}$, O(8)$^{(b)}$, and O(10w) set of atoms build the equatorial plane at Co(1) whereas the axial positions are filled by O(9w) and O(6). In the case of Co(2) and Co(3), the equatorial plane is formed by O(2) O(2)$^{(c)}$, O(9w), and O(9w)$^{(c)}$ and O(4), O(4)$^{(e)}$, O(11w), and O(11w)$^{(e)}$, respectively. The axial positions occupied by O(7)$^{(b)}$ and O(7)$^{(d)}$ for Co(2) and O(1) and O(1)$^{(e)}$ for Co(3). The values


dx.doi.org/10.1021/ic500443t | *Inorg. Chem.* XXXX, XXX, XXX−XXX

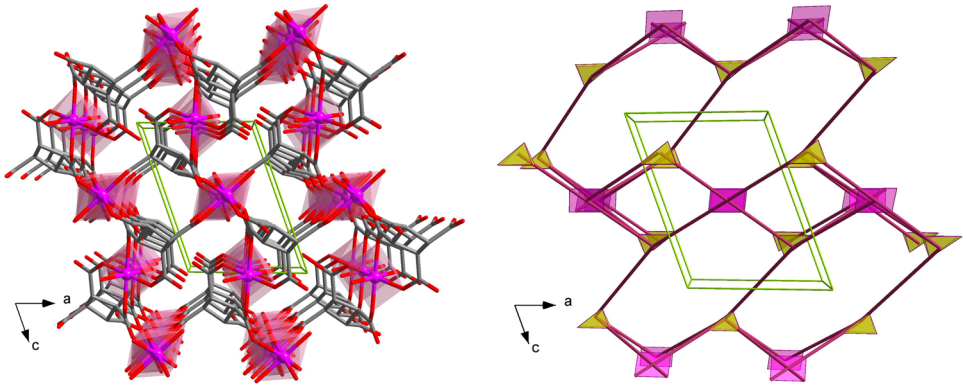


**Figure 4.** (Left) Perspective view along the crystallographic *b*-axis of a fragment of the structure of **1**, showing how the *bc*-layers are pillared along the *a*-axis. The hydrogen atoms have been omitted for sake of clarity. (Right) Topological scheme of **1**, where the pink and yellow polyhedra represent the 4- (cobalt) and 5-fold ($cbut^{4-}$) nodes, respectively.

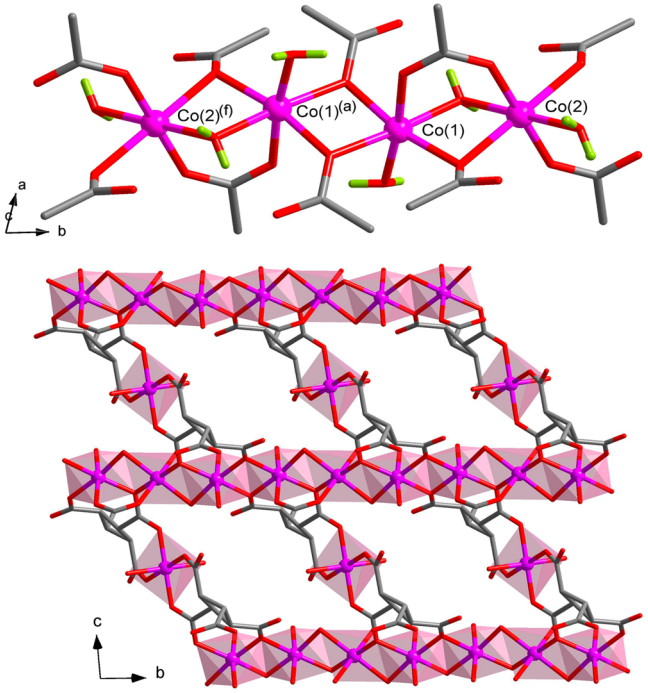


**Figure 5.** (Top) View of a fragment of the regular alternating chain of cobalt(II) ions running along the crystallographic *b*-axis. The hydrogen atoms of the water molecules are depicted in light green color. Symmetry code: (f) $x, y - 1, z$. (Bottom) Projection view down the *a*-axis of the *bc*-layers showing the interchain connection through the third crystallographically independent Co(3) center.

of $\phi$ and $s/h$ parameters are 64.14 and 1.14 [Co(1)], 56.37 and 1.13 [Co(2)] and 63.72° and1.11 [Co(3)] (to be compared to 60° and 1.22 for an ideal octahedron).[27] The average values of the equatorial bond lengths at Co(1), Co(2), and Co(3) are 2.081(2), 2.146(2) and 2.135(2) Å respectively, whereas the mean axial bond lengths are 2.095(2), 1.994(2), and 2.030(2) Å for Co(1), Co(2), and Co(3), respectively (see Table 2).

A crystallographically independent fully deprotonated $cbut^{4-}$ ligand in *trans*−*trans*−*trans* conformation is present in **1**. Its cyclobutane ring exhibits a puckered conformation with values of 19.39(2)° and 19.58(2)° for the dihedral angles between the C(2)C(3)C(4) and C(3)C(4)C(5) and C(2)C(3)C(5) and C(2)C(4)C(5) planes, respectively. This structural feature is in agreement with the Margulis rule, which establish that the noncentrosymmetric substituted rings are always puckered whereas the centrosymmetric ones may be or not.[28] The $cbut^{4-}$ ligand adopts simultaneously the *bis-bidentate* [through the O(1) and O(4) atoms toward Co(1) and across the O(2) and O(6) atoms toward Co(3)] and as *tetrakis-monodentate* [through O(2), O(6), O(7), and O(8) atoms toward Co(2), $Co(1)^{(c)}$, $Co(2)^{(g)}$, and $Co(1)^{(g)}$, respectively] coordination modes (see Figure 2).

There is an extensive network of hydrogen bonds, involving all the hydrogen atoms of the coordination water molecules [O(9w), O(10w), and O(11w)] and the oxygen atoms from carboxylate groups of the cbut ligand with values of the $O_w\cdots O$ distance and $O_w-H\cdots O$ angle covering the ranges 2.6583−3.0102 Å and 145.1−177.2°.

**Magnetic Study of 1.** The magnetic properties of **1** in the form of both $\chi_M$ and $\chi_M T$ versus $T$ plots [$\chi_M$ is the magnetic susceptibility per two Co(II) ions] under applied dc fields of 5000 and 1000 Oe are shown in Figure 6 (left). $\chi_M T$ at room temperature is 6.3 $cm^3\ mol^{-1}\ K$ [$\mu_{eff}$ per one Co(II) = 5.03 $\mu_B$], a value which is greater than the expected for the spin-only formula [$\mu_{eff}$ = 3.87 $\mu_B$ for $S = 3/2$ with $g = 2.0$], indicating that the distortion of the octahedral symmetry of the cobalt(II) ions in **1** is not so large as to induce the total quenching of the $^4T_{1g}$ ground state. Upon cooling, $\chi_M T$ slightly decreases to reach a minimum value of 5.6 $cm^3\ mol^{-1}\ K$ at ∼14 K. At lower temperatures, $\chi_M T$ sharply increases to 14.3 $cm^3\ mol^{-1}\ K$ at 5.0 K and it finally decreases to 0.44 $cm^3\ mol^{-1}\ K$ at 1.9 K. This increase of $\chi_M T$ in the low temperatures domain is field-dependent as shown in the inset of Figure 6 (left). A maximum of the magnetic susceptibility is observed at 5.0 K under applied dc fields smaller than 1500 Oe (the critical field $H_c$). All these features can be interpreted as follow: (i) the fact that the value of $\chi_M T$ at the minimum (∼5.6 $cm^3\ mol^{-1}\ K$ at 14 K) is well above than that calculated for two magnetically isolated cobalt(II) ions [3.5 $cm^3\ mol^{-1}\ K$, each Co(II) having $S_{eff}$ = 1/2 and $g \approx 4.3$][5,29] and the further increase of $\chi_M T$, unambiguously support the occurrence of a ferromagnetic interaction between the Co(II) ions (the decrease of $\chi_M T$ in the high temperature region being due to spin−orbit coupling effects);[5b] (ii) the presence of a maximum in the magnetic susceptibility curve is due to an antiferromagnetic ordering; and (iii) the field-dependence of this maximum, which disappears for applied magnetic-fields larger than 1500 Oe ($H_c$) corresponds to a metamagnetic behavior,[30] the value of $H_c$ being given by the inflection point of the magnetization plot at


dx.doi.org/10.1021/ic500443t | Inorg. Chem. XXXX, XXX, XXX−XXX

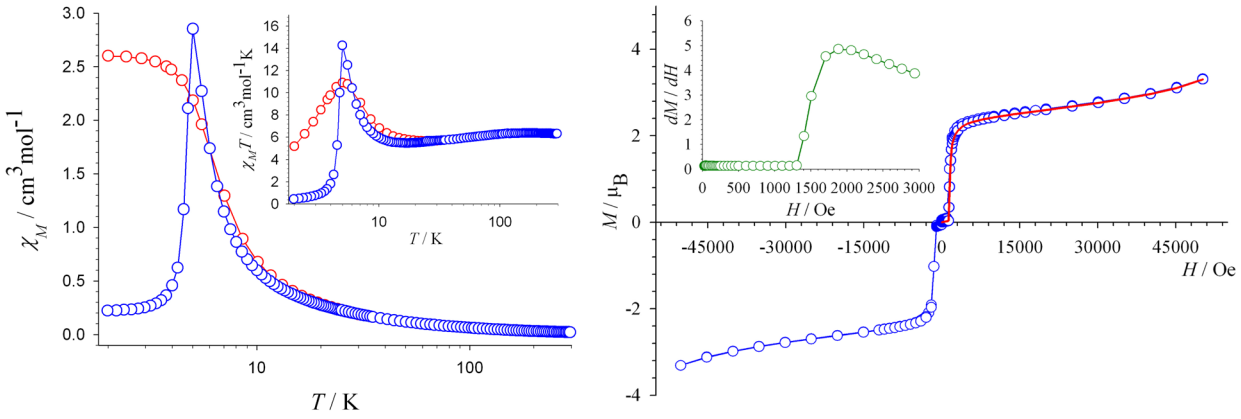


**Figure 6.** (Left) Thermal variation of the susceptibility under magnetic applied fields of 1000 (blue circles) and 5000 Oe (red circles). The inset shows the temperature dependence of $\chi_M T$ under the same magnetic fields. The temperature axes have been represented in a logarithmic scale for the sake of the clarity of the low temperature region. (Right) Isothermal magnetization plot at 2.0 K. The solid red line represent the first magnetization. Inset: d$M$/d$H$ vs $H$.

2.0 K [see Figure 6 (left)]. Neutron diffraction experiments at temperatures below 5.0 K confirm the occurrence of this antiferromagnetic ordering (see below).

The magnetization curve measured at 2.0 K shows a sigmoidal shape characteristic of a metamagnetic behavior [Figure 6 (right) and Supporting Information Figure S3]. The magnetization remains almost constant under applied magnetic fields ranging from 0 to 1500 Oe; this feature supports the occurrence of an overall antiferromagnetic behavior. For applied magnetic fields above ~1500 Oe ($H_c$), the magnetization value increases abruptly reaching a value of 2.3 $\mu_B$ at 5000 Oe which coincides with the saturation value of the field-cooled susceptibility curve [$M \approx 13000$ cm$^3$ mol$^{-1}$ Oe $\approx 2.3$ $\mu_B$ in Figure 6 (left)]. This value is about half of the expected saturation magnetization for two Co(II) ions, suggesting the occurrence of ferrimagnetic planes. This behavior could be understood as a magnetic phase transition from antiferromagnetic order to a field-induced ferrimagnetic state (metamagnetic behavior). This metamagnetic phase transition has been confirmed with the field dependence of the ac susceptibility measurements at 3 and 4 K (see Supporting Information Figure S4). In fact, the magnetization curve increases linearly with the applied field, as expected for a ferrimagnetic compound and a change in the curvature of the magnetization is observed for external magnetic field higher than 40000 Oe. This feature is compatible with the beginning of a second metamagnetic transition, where the remnant antiferromagnetic interactions within the ferrimagnetic layers start to be overcome reaching 3.3 $\mu_B$ at 50 kOe, a value which is far from that expected for two isolated cobalt(II) ions. A small hysteresis loop is also observed at low applied fields with a coercive field of ~40 Oe (see Supporting Information Figure S2).

On the basis of the temperature-dependence of the critical magnetic field of metamagnetism obtained from the previous results (see Figure S5), we are able to determine the magnetic phase diagram of this compound (see Figure 7), where three different regions: paramagnetic above 5 K, antiferromagnetic and field-induced ferromanetic below 5 K, can be distinguish.

Having in mind the structure of **1**, four pathways could be involved in the magnetic exchange: (A) the double $\mu$-oxo(carboxylate) bridge between Co(1) and Co(1)$^{(a)}$ with a Co(1)−O(6)−Co(1)$^{(a)}$ angle equal to 96.8°; (B) the aqua [Co(1)−O(9w)−Co(2) angle of 96.1°], single oxo-

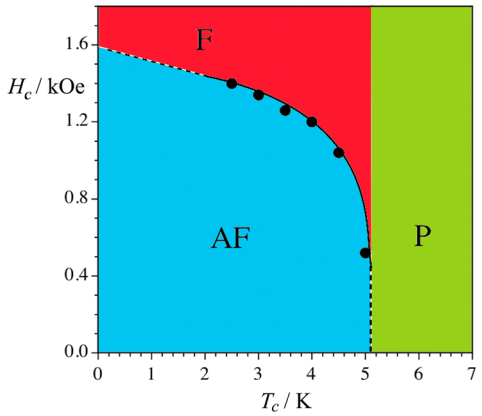


**Figure 7.** Magnetic phase diagram for **1**, where three different regions have been represented, paramagnetic (green), antiferromagnetic (blue), and field induced ferromagnetic phase (red). The solid black circles have been obtained deriving the M vs H curves (Supporting Information Figure S5).

(carboxylate) [Co(1)−O(2)−Co(2) angle of 96.6°] and *syn*−*syn* carboxylate bridges between Co(1) and Co(2); (C) the *anti*−*anti* Co(1)−O(2)−C(7)−O(1)−Co(3) and *anti*−*syn* Co(2)−O(2)−C(7)−O(1)−Co(3); and (D) those through the skeleton of the cbut$^{4-}$ ligand with a shortest cobalt−cobalt distance of 7.028(2) Å [Co(1)−O(6)−C(6)−C(5)−C(3)−C(8)−O(7)−Co(2)$^{(g)}$ pathway]. The much longer cobalt−cobalt separation in D (~7.0 Å) when compared to the other three (~3.1 Å in A and B and 5.7 and 4.9 Å in C] allows us to neglect the magnetic exchange pathway D. Previous magneto-structural studies have shown the occurrence of significant ferromagnetic interactions between Co(II) ions through the pathways A and B supporting the presence in **1** of ferromagnetic chains along the crystallographic *b*-axis.[13b,30] An antiferromagnetic coupling through the *anti*−*anti* carboxylate bridge of the pathway C would lead to a non-compensation of the magnetic moments within each *bc*-layer, giving a ferrimagnetic plane. Finally, a weak antiferromagnetic interlayer interaction through the crystallographic *a*-axis (dipolar interactions and/or an exchange through the long cbut$^{4-}$ ligand) accounts for the antiferromagnetic ordering (metamagnetic behavior with $H_c$ = 1500 Oe). This hypothesis


dx.doi.org/10.1021/ic500443t | *Inorg. Chem.* XXXX, XXX, XXX−XXX

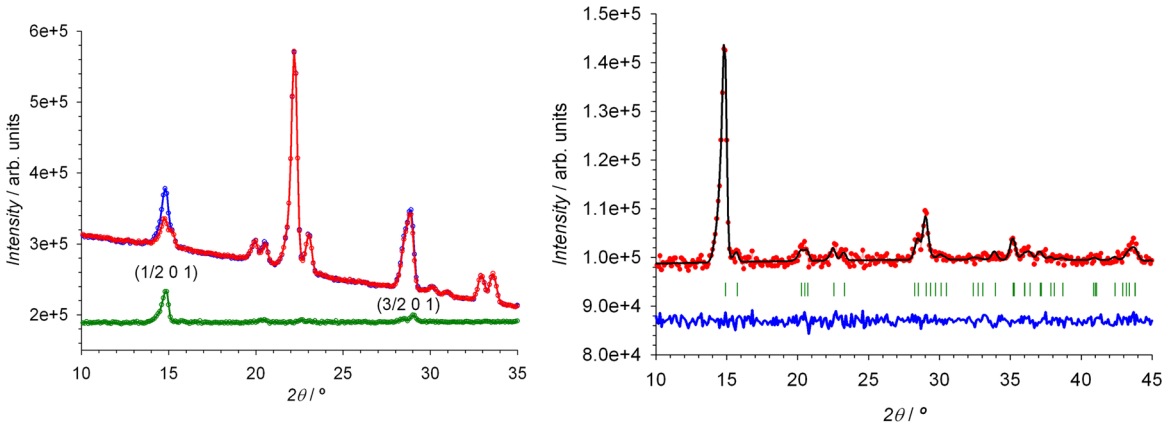


**Figure 8.** (Left) Neutron powder patterns of **1** collected at 2.0 (blue line) and 10 K (red line) using a D20 diffractometer. The difference diffraction pattern with the selected (1/2 0 1) and (3/2 0 1) magnetic reflections corresponds to the green line. These reflections are due to the contribution of the magnetic phase (see text). (Right) Fit of the difference pattern with the $\Gamma_2$ irrep and the (1/2, 0, 0) magnetic propagation vector (see text).

about the magnetic structure have been confirmed by neutron diffraction measurements at low temperatures (see hereunder).

**Magnetic Structure of 1.** Aiming at determining the magnetic structure of **1** under zero applied magnetic field below the ordering temperature ($T_N \approx 5.0$ K), a series of neutron diffraction experiments at different temperatures above and below $T_N$ were carried out by using the D20 powder diffractometer. The high flux neutron diffraction pattern collected in the paramagnetic phase (∼10 K) was used to refine the low temperature structural model (see Supporting Information Figure S6). The Rietveld refinement was carried out using, as a starting point, the crystal structure obtained from the D2B measurements at 300 K (see the neutron nuclear structure refinement section). The increase of intensity on some Bragg reflections in the neutron diffraction pattern at 2.0 K suggests the occurrence of a long-range magnetic ordering (see Supporting Information Figure S7), which is in agreement with the dc magnetic measurements. It should be noted that the magnetic contribution can be observed only at low angles, while the remaining reflections (nuclear ones) keep constant their intensity (except from the Debye−Waller factor) in the whole temperature range explored. The lack of extra intensity on top of the nuclear reflections indicates that the magnetic structure is strictly antiferromagnetic. Because of the weak magnetic contribution, the partial overlap between nuclear and magnetic reflections, and the background produced by the high number of hydrogen atoms in the sample, the refinement of the magnetic structure directly from this pattern gave a nonaccurate result. A different strategy was followed in order to handle these difficulties. First, we subtracted the normalized nuclear intensity of the paramagnetic phase (∼10 K) from the low temperature pattern (∼2.0 K). This difference pattern isolates the magnetic contribution and therefore, a more accurate indexing of the magnetic reflections, as well as the magnetic structure determination can be undertaken. The intensity of the calculated difference pattern has been shifted to an arbitrary value of ∼100 000 units to achieve a similar background than those observed in the original patterns (see Figure 8).

The indexing of the observed magnetic reflections in the difference pattern was done using the k-Search program included in the FullProf suite.[31] The only solution compatible with the magnetic reflections observed in the difference pattern give rise to the propagation vector **k** = (1/2, 0, 0). The representational analysis technique described by Bertaut has been used to determine the possible magnetic structures compatible with the $P\bar{1}$ space group of **1**.[32] The propagation vector group $G_k$ (little group) coincides with the space group $P\bar{1}$. Two irreducible one-dimensional representations of the group $G_k$, $\Gamma_1$, and $\Gamma_2$ and a simple set of basis vectors for each irreducible representation can be trivially determined. They have been verified with the help of the BASIREPS program.[33] The representational analysis provides the expression of the Fourier vector coefficients as linear combinations of basis functions. The basis vectors describe the possible arrangements of magnetic structures.

A detailed basis vectors for both irreducible representations (irreps) is shown in Table 3. The magnetic representation $\Gamma_M$ for each magnetic site [Wyckoff position 2*i* for Co(1), 1*h* for Co(2), and 1*e* for Co(3)] can be decomposed as direct sum of irreps by applying the great orthogonality theorem. Each irrep $\Gamma_1$ and $\Gamma_2$ appear three-times for the site 2*i* whereas for the site 1*h* and 1*e* only $\Gamma_2$ is present three-times.

**Table 3. Irreducible Representations (Irreps) Γ of the Little Group $G_k = P - 1$ and Basis Vectors of the Two Irreducible Representations for the Sites[a] Co(2*i*) = 0.4153, 0.1804, 0.5366; Co(1*h*) = 0.5, 0.5, 0.5; and Co(1*e*) = 0.5, 0.5, 0**

| irreps | | *x*, *y*, *z* | −*x*, −*y*, −*z* |
|---|---|---|---|
| $\Gamma_1$ | | 1 | 1 |
| $\Gamma_2$ | | 1 | −1 |
| | | basis vectors | |
| $\Gamma_1$ | Co(2*i*) | {(100),(010),(001)} | {(100),(010),(001)} |
| | Co(1*h*) | {(100),(010),(001)} | |
| | Co(1*e*) | {(100),(010),(001)} | |
| | Co(2*i*) | {(100),(010),(001)} | {(1̄00),(01̄0),(001̄)} |
| $\Gamma_2$ | Co(1*h*) | {(100),(010),(001)} | |
| | Co(1*e*) | {(100),(010),(001)} | |

[a]Note that the magnetic sites of the cobalt atoms: (2*i*), (1*h*), and (1*e*) correspond to Co(1), Co(2), and Co(3), respectively.

$$\Gamma_{2i} = 3\Gamma_1 \oplus 3\Gamma_2 \quad (1)$$

$$\Gamma_{1h} = 3\Gamma_2 \quad (2)$$

$$\Gamma_{1e} = 3\Gamma_2 \quad (3)$$

The magnetic moments for site 2*i* of the two sublattices are obtained from the basis vectors as $\mathbf{m}_{2i}(1) = (u, v, w)$ and $\mathbf{m}_{2i}(2)$


dx.doi.org/10.1021/ic500443t | Inorg. Chem. XXXX, XXX, XXX−XXX

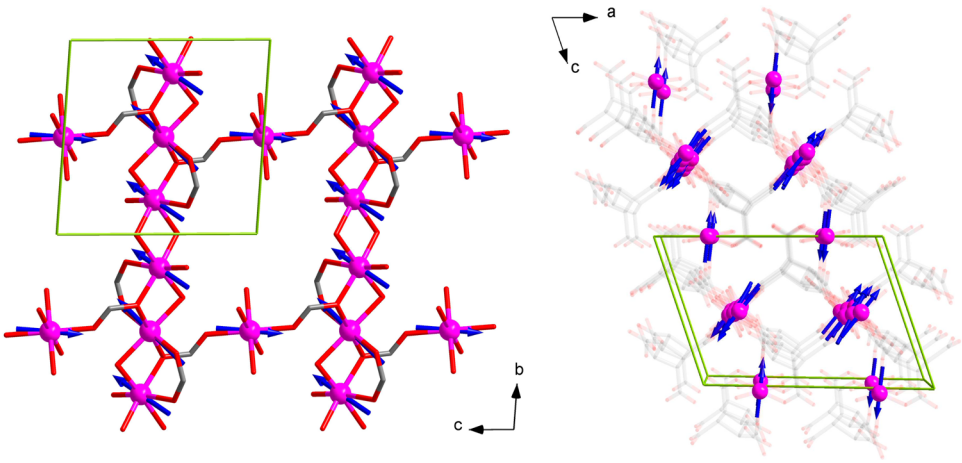


**Figure 9.** (Left) View of the organic–inorganic *bc*-layer together with the magnetic moments for each magnetic site. Hydrogen atoms and the skeleton of the cbut$^{4-}$ ligand have been omitted for clarity. (Right) Projection along the *b*-axis of the nuclear and magnetic structure of **1**. Nonmagnetic atoms have been represented in transparence model and the hydrogen atoms have been omitted for the sake of clarity. The magnetic unit cell has been represented in light-green in both figures.

= $(u, v, w)$ for irrep $\Gamma_1$ and $\mathbf{m}_{2i}(1) = (u, v, w)$ and $\mathbf{m}_{2i}(2) = (-u, -v, -w)$ for irrep $\Gamma_2$ whereas for the site 1*h* and 1*e* the magnetic moments are given by $\mathbf{m}_{1h} = (p, q, r)$ and $\mathbf{m}_{1e} = (k, l, m)$. In both cases there are nine degrees of freedom $(u, v, w, p, q, r, k, l, m)$ for the magnetic structure. The Shubnikov group corresponding to $\Gamma_1$ is $P_{2s}1$ and that corresponding to $\Gamma_2$ is $P_{2s}-1$ [in Opechowski–Guccione notation].[34] Under the assumption that the all sublattices described by $\Gamma_1$ and $\Gamma_2$ are ordered, the magnetic structure can only be described by irrep $\Gamma_2$. This is due to the fact that $\Gamma_1$ is contained neither in $\Gamma_{1h}$ nor in $\Gamma_{1e}$. Moreover $\Gamma_2$ is the only irrep that provides a satisfactory agreement between the calculated and the experimental diffraction pattern collected below $T_N$. From the Rietveld refinement of the difference pattern we are able to obtain the relative orientation of the magnetic moments of the three magnetic sites present in this compound.

Keeping in mind the crystal structure of **1**, let us describe its magnetic structure. The Co(1) atoms [magnetic site (2*i*)], which are connected between them through a double *μ*-oxo(carboxylate) bridge (pathway A), are ferromagnetically coupled. These dinuclear units are connected between them through the Co(2) atom [magnetic site (1*h*)] involving three different bridges, the *μ*-oxo(carboxylate), the *μ*-aqua and the *syn–syn* carboxylate bridge (pathway B), giving rise to the ··· Co(2)–Co(1)–Co(1)–Co(2)–Co(1)··· chains which are extended along the *b*-axis. The interaction between the Co(1) and the Co(2) atoms has a remarkable ferromagnetic character as can be seen in Figure 9. Each chain is connected to the adjacent one through the Co(3) [magnetic site (1*e*)] atom, which acts as connector through two carboxylate bridges in *trans*-coordination (pathway C). The Co(II)–Co(II) interaction through this bridge has an antiferromagnetic behavior, as expected for the presence of an *anti–anti* carboxylate bridge. The modulus of the resultant magnetization within the *bc*-layers calculated for a molecular unit [$\mathbf{M} = (2\mathbf{m}_{2i} + \mathbf{m}_{1h} + \mathbf{m}_{1e})/2$] is approximately 3.2(3) $\mu_B$. The refined values of the magnetic moment of each cobalt atoms are shown in Table 4. It is interesting to note that in the case of an isotropic ferrimagnetic plane, where all the magnetic moments are collinear to each other (parallel or antiparallel), the expected magnetic moment per formula unit (two cobalt atoms) of such a plane would be the corresponding for one Co(II) ion (about 2.9 $\mu_B$, see Table 4). However, the experimental value (3.2 $\mu_B$) is slightly larger. This fact is related to the high local anisotropy of the Co(II) ions which produces a significant departure from collinearity (canting of the magnetic moments). The angle between the magnetic moments of the Co(1) and Co(3) ions is about 155° denoting an antiferromagnetic character, nevertheless this canting avoids the complete cancellation of both magnetic moments. The angle between the magnetic moments of the Co(1) and Co(2) ions is smaller (~12°), being basically collinear (see Supporting Information Figure S8). It is also interesting to observe the direction of the magnetic moments on the Co(II) ions within the structural framework. In the case of Co(2) and Co(3), their magnetic moments are slightly tilted from the axis that connect the *trans* positioned carboxylate-oxygens [O(7) and O(7)$^{(g)}$ for Co(2) and O(1) and O(1)$^{(e)}$ for Co(3)] while for the Co(1) atom, the magnetic moment is most likely parallel to the normal of the plane formed by O(2), O(9w), and O(10w) (see Supporting Information Figure S9).

**Table 4. Magnetic Moment Components for Each Metal Site at 2.0 K for (1)$^{a,b}$**

| | $M_a$ | $M_b$ | $M_c$ | $M_{Total}$ |
|---|---|---|---|---|
| Co(2*i*) | −2.62(14) | 1.2(3) | 1.67(14) | 2.56(10) |
| Co(1*h*) | −2.9(3) | 2.3(3) | 2.40(18) | 3.39(20) |
| Co(1*e*) | 1.78(19) | −0.24(1) | −3.04(18) | −2.95(14) |

$^a$The components (in $\mu_B$) are given with respect to the unit vectors along the crystallographic *a*, *b*, and *c* axes. $^b$Note that the magnetic sites of the cobalt atoms, (2*i*), (1*h*), and (1*e*), correspond to Co(1), Co(2), and Co(3), respectively.

These ferrimagnetic layers are antiferromagnetically coupled along the *a*-axis: an antitranslation operation is applied along the *a*-axis because of the occurrence of a propagation vector $\mathbf{k} = (1/2, 0, 0)$ [Figure 9 (right)]. The saturation value of the magnetization of the metamagnetic phase (for $H > H_c$) corresponds approximately with one cobalt ion [see Figure 6]. The interpretation of this result based on the zero field neutron diffraction experiments is not straightforward, because a wide number of different scenarios can be envisaged. The most plausible explanations involve the change of the propagation vector from $\mathbf{k} = (1/2, 0, 0)$ to $\mathbf{k} = (0, 0, 0)$ or the presence of two simultaneous propagation vectors which allow the


dx.doi.org/10.1021/ic500443t | *Inorg. Chem.* XXXX, XXX, XXX–XXX

occurrence of a net ferromagnetic state, which is not permitted with the **k** = (1/2, 0, 0).

The determination of the magnetic structure of the field-induced ferromagnetic phase (for $H > H_c$) was not possible because of the small size of the single crystals of **1**, and our attempts to grow a suitable single crystals for neutron diffraction experiments (~1 $mm^3$) were unsuccessful.

## CONCLUSIONS

In this work, we have presented a new metal−organic network of formula $[Co_2(cbut)(H_2O)_3]_n$ obtained by using the well-known hydrothermal technique. The single crystals were structurally characterized through synchrotron X-ray diffraction at 100 K resulting in a 3D pillared layer network. The magnetization versus magnetic applied field data shows a ferromagnetic field-induced phase transition under magnetic fields above the 1500 Oe, as well as a small hysteresis loop at low magnetic fields. Susceptibility measurements support a metamagnetic behavior and suggest an antiferromagnetic order for temperatures below ~5 K. To obtain the magnetic structure we have performed neutron diffraction experiments. First, the structural model of $[Co_2(cbut)(H_2O)_3]_n$ compound were refined from neutron data at 300 K allowing the localization of the hydrogen atoms. Second, the 10 K refined data was used to locate the position of the atoms at low temperatures, as well as to fix the structural contribution to be used as starting point for the refinement of the magnetic structure. Finally, the neutron diffraction data at 2.0 K support the antiferromagnetic order suggested by the magnetic susceptibility measurements and were used to calculate the difference pattern, between the 10 and 2.0 K to isolate the magnetic contribution.

The propagation vector found was **k** = (1/2, 0, 0) and the only irreducible representation fitting the experimental data describes a noncompensate antiferromagnetic arrangement of the magnetic moments within the *bc*-layers, which are antiferromagnetically coupled along the *a*-axis. This configuration fits very well with the experimental data and supports the macroscopic behavior described by the susceptibility measurements.

The angle between the magnetic moments of the three independent cobalt ions in the structure of **1** were analyzed and correlated with the proposed exchange pathways A, B, and C. The well-known ferromagnetic A and B bridges lead to almost collinear moments between Co(1) themselves, and Co(1) and Co(2). However, the weak antiferromagnetic interactions (through the C pathway) between the ferromagnetic chains do not align the moments completely antiparallel, forming noncompensated planes. The theoretical calculations of the interactions through these bridges in **1** are in progress.

## ASSOCIATED CONTENT

### Supporting Information

Structure determination and refinement details, X-ray crystallographic data in CIF format, neutron thermodiffractogram collected at D20 diffractometer from 15 to 2 K, magnetic hysteresis loop at 2 K, Rietveld refinement of the neutron diffraction pattern (D20) collected at 2.0 and 10.0 K and comparative of the atomic coordinates obtained from low temperature synchrotron measurement (100 K) collected at BM16 and those refined from high-resolution neutron diffraction at RT obtained from D2B data. This material can be found free of charge via the Internet at http://pubs.acs.org.

## AUTHOR INFORMATION

### Corresponding Authors

*E-mail: fabelo@ill.fr.

*E-mail: jpasang@ull.edu.es.

### Notes

The authors declare no competing financial interest.

## ACKNOWLEDGMENTS

The authors are grateful to the ILL instruments for the neutron beam-time allocated. Partial funding for this work is provided by the Ministerio Español de Ciencia e Innovación through projects MAT2010-16981, CTQ2010-15364, DPI2010-21103-C04-03, MAT2011-27233-C02-02, MAT2011-25991 and "Factoría de Cristalización" (Consolider-Ingenio2010, CSD2006-00015), the Generalitat Valenciana (ISIC/2012/002), and the CEI Canarias: Campus Atlántico Tricontinental. P.D.-G. also thanks to Ministerio Español de Economia y Competitividad through FPI program for predoctoral contracts.

## DEDICATION

Dedicated to Professor Dr. Marius Andruh on the occasion of his 60th birthday.

## REFERENCES

(1) (a) Miller, J. S.; Gatteschi, D. *Chem. Soc. Rev.* **2011**, *40*, 3065−3066 and references therein.. (b) Hicks, R. G. *Nat. Chem.* **2011**, *3*, 189−191. (c) Urdampilleta, M.; Klyatskaya, S.; Cleuziou, J.-P.; Ruben, M.; Wernsdorfer, W. *Nat. Mater.* **2011**, *10*, 502−506. (d) Pal, S. K.; Bag, P.; Sarkar, A.; Chi, X.; Itkis, M. E.; Tham, F. S.; Donnadieu, B.; Haddon, R. C. *J. Am. Chem. Soc.* **2010**, *132*, 17258−17264. (e) Shatruk, M.; Avendano, C.; Dunbar, K. R. *Prog. Inorg. Chem.* **2009**, *56*, 155−334. (f) Bogani, L.; Wernsdorfer, W. *Nat. Mater.* **2008**, *7*, 179−186. (g) Gruselle, M.; Train, C.; Boubekeur, K.; Gredin, P.; Ovanesyan, N. *Coord. Chem. Rev.* **2006**, *250*, 2491−2500. (h) Rabu, P.; Drillon, M.; Awaga, K.; Fukita, W.; Sekine, T. In *Magnetism: Molecules to Materials*' Miller, J. S.; Drillon, M., Eds.; Wiley-VCH, Weinheim, Germany, 2001; p 357. (i) Verdaguer, M.; Bleuzen, A.; Marvaud, V.; Vaissermann, J.; Seuleiman, M.; Desplanches, C.; Scuiller, A.; Train, C.; Garde, R.; Gelly, G.; Lomenech, C.; Rosenman, I.; Veillet, P.; Cartier, C.; Villain, F. *Coord. Chem. Rev.* **1999**, *1023*, 190−192. (j) Coronado, E.; Delhaes, P.; Gatteschi, D.; Miller, J. S. *Molecular Magnetism: From Molecular Assemblies to the Device*, NATO ASI Series; NATO: Washington DC, 1995.

(2) (a) Moulton, B.; Zaworotko, M. J. *Chem. Rev.* **2001**, *101*, 1629−1658. (b) Brammer, L. *Chem. Soc. Rev.* **2004**, *33*, 476−489. (c) Biradha, K.; Sarkar, M.; Rajput, L. *Chem. Commun.* **2006**, 4169−4179.

(3) (a) Chen, J.; Liu, P.-W.; Li, C.-P. *Inorg. Chem. Commun.* **2013**, *36*, 105−108. (b) Lago, A. B.; Carballo, R.; Rodríguez-Hermida, S.; Vázquez-López, E. M. *CrystEngComm* **2013**, *15*, 1563−1570. (c) Fang, R. Q.; Zhang, X. M. *Inorg. Chem.* **2006**, *45*, 4801−4810.

(4) Kurmoo, M. *Chem. Soc. Rev.* **2009**, *38*, 1353−1379.

(5) (a) Figgis, B. N.; Hitchman, M. A. *Ligand Field Theory and Its Applications*; Wiley-VCH: New York, 2000. (b) Lloret, F.; Julve, M.; Cano, J.; Ruiz-García, R.; Pardo, E. *Inorg. Chim. Acta* **2008**, *361*, 3432−3445.

(6) Vallejo, J.; Castro, I.; Ruiz-García, R.; Cano, J.; Julve, M.; Lloret, F.; De Munno, G.; Wernsdorfer, W.; Pardo, E. *J. Am. Chem. Soc.* **2012**, *134*, 15704−15707.

(7) (a) Murrie, M. *Chem. Soc. Rev.* **2010**, *39*, 1986−1995. (b) Gatteschi, D.; Sessoli, R.; Villain, J. *Molecular Nanomagnets*; Oxford University Press: Oxford, U.K, 2006. (c) *Single-Molecule Magnets and Related Phenomena, Structure and Bonding*; Winpenny, R., Ed.; Springer: Berlin, 2006; Vol. *122*.

(8) (a) Sun, H. L.; Wang, Z. M.; Gao, S. *Coord. Chem. Rev.* **2010**, *254*, 1081−1100. (b) Miyasaka, H.; Julve, M.; Yamashita, M.; Clérac, R.

*Inorg. Chem.* **2009**, *48*, 3420−3437. (c) Bogani, L.; Vindigni, A.; Sessoli, R.; Gatteschi, D. *J. Mater. Chem.* **2008**, *18*, 4750−4758.
(9) (a) Pasán, J.; Delgado, F. S.; Rodríguez-Martín, Y.; Hernández-Molina, M.; Ruiz-Pérez, C.; Sanchíz, J.; Lloret, F.; Julve, M. *Polyhedron* **2003**, *22*, 2143−2153. (b) Rodríguez-Fortea, A.; Alemany, P.; Alvarez, S.; Ruiz, E. *Chem.—Eur. J.* **2001**, *7*, 627−637. (c) Colacio, E.; Domínguez-Vera, J. M.; Ghazi, M.; Kivekäs, R.; Klinga, M.; Moreno, J. M. *Eur. J. Inorg. Chem.* **1999**, 441−445. (d) Kato, M.; Muto, Y. *Coord. Chem. Rev.* **1988**, *92*, 45−83.
(10) Jia, P. H.; Li, W.; Hu, Z. F.; Zhang, J. *Eur. J. Inorg. Chem.* **2006**, 4264−4270.
(11) (a) Kumagai, H.; Oka, Y.; Inoue, K.; Kurmoo, M. *J. Phys. Chem. Solids* **2004**, *65*, 55−60. (b) Rueff, J. M.; Masciocchi, N.; Rabu, P.; Sironi, A.; Skoulios, A. *Eur. J. Inorg. Chem.* **2001**, 2843−2848.
(12) (a) Mishra, V.; Lloret, F.; Mukherjee, R. *Inorg. Chim. Acta* **2006**, *359*, 4053−4062. (b) Rueff, J. M.; Paulsen, C.; Souletie, J.; Drillon, M.; Rabu, P. *Solid State Sci.* **2005**, *7*, 431−436. (c) Delgado, F. S.; Hernández-Molina, M.; Sanchiz, J.; Ruiz-Pérez, C.; Rodríguez-Martín, Y.; López, T.; Lloret, F.; Julve, M. *CrystEngComm.* **2004**, *6*, 106−111. (d) Delgado, F. S.; Sanchiz, J.; Ruiz-Pérez, C.; Lloret, F.; Julve, M. *CrystEngComm* **2003**, *5*, 280−284. (e) Lee, E.; Kim, Y. J.; Jung, D. Y. *Inorg. Chem.* **2002**, *41*, 501−506. (f) Kumagai, H.; Oka, Y.; Inoue, K.; Kurmoo, M. *Dalton Trans.* **2002**, 3442−3446.
(13) (a) Fabelo, O.; Pasán, J.; Cañadillas-Delgado, L.; Delgado, F. S.; Lloret, F.; Julve, M.; Ruiz-Pérez, C. *Inorg. Chem.* **2009**, *48*, 6086−6095. (b) Fabelo, O.; Cañadillas-Delgado, L.; Pasán, J.; Delgado, F. S.; Lloret, F.; Cano, J.; Julve, M.; Ruiz-Pérez, C. *Inorg. Chem.* **2009**, *48*, 11342−11351.
(14) (a) Feyerherm, R.; Loose, A.; Rabu, P.; Drillon, M. *Solid State Chem.* **2003**, *5*, 321−326. (b) Rabu, P.; Rueff, J. M.; Huang, Z. L.; Angelov, S.; Soulette, J.; Drillon, M. *Polyhedron* **2001**, *20*, 1677−1685. (c) Kurmoo, M.; Kumagai, H.; Green, M. A.; Lovett, B. W.; Blundell, S. J.; Ardavan, A.; Singleton, J. *J. Solid State Chem.* **2001**, *159*, 343−351.
(15) (a) Jia, H. P.; Li, W.; Hu, Z. F.; Zhang, J. *Inorg. Chem. Commun.* **2007**, *10*, 265−268. (b) Lü, Z. L.; Chen, W.; Xu, J. Q.; Zhang, L. J.; Pan, C. L.; Wang, T. G. *Inorg. Chem. Commun.* **2003**, *6*, 244−248. (c) Platter, M. J.; Foreman, M. R. S.; Howie, J. R. A.; Skakle, J. M. S.; Slawin, A. M. Z. *Inorg. Chim. Acta* **2001**, *315*, 126−132.
(16) (a) Fabelo, O.; Cañadillas-Delgado, L.; Pasán, J.; Díaz-Gallifa, P.; Ruiz-Pérez, C.; Lloret, F.; Julve, M.; Puente Orench, I.; Campo, J.; Rodríguez-Carvajal, J. *Inorg. Chem.* **2013**, *52*, 12818−12827. (b) Fabelo, O.; Pasán, J.; Cañadillas-Delgado, L.; Delgado, F. S.; Yuste, C.; Lloret, F.; Julve, M.; Ruiz-Pérez, C. *CrystEngComm* **2009**, *11*, 2169−2179. (c) Fabelo, O.; Pasán, J.; Cañadillas-Delgado, L.; Delgado, F. S.; Lloret, F.; Julve, M.; Ruiz-Pérez, C. *Inorg. Chem.* **2008**, *47*, 8053−8061. (d) Fabelo, O.; Pasán, J.; Lloret, F.; Julve, M.; Ruiz-Pérez, C. *Inorg. Chem.* **2008**, *47*, 3568−3576. (e) Fabelo, O.; Pasán, J.; Lloret, F.; Julve, M.; Ruiz-Pérez, C. *CrystEngComm* **2007**, *9*, 815−827. (f) Majunder, A.; Gramlich, V.; Rosair, G. M.; Batten, S. R.; Masuda, J. S.; El Fallah, M. S.; Ribas, J.; Sutter, J. P.; Desplanches, C.; Mitra, S. *Cryst. Growth Des.* **2006**, *6*, 2355−2368. (g) Kumagai, H.; Kepert, C. J.; Kurmoo, M. *Inorg. Chem.* **2002**, *41*, 3410−3422. (h) Gutschke, S. O. H.; Price, D. J.; Powell, A. K.; Wood, P. T. *Eur. J. Inorg. Chem.* **2001**, 2739−2741. (i) Rochon, F. D.; Massarweh, G. *Inorg. Chem. Acta* **2000**, *304*, 190−198. (j) Karanovic, L.; Poleti, D.; Bogdanovic, G. A.; Spasojevic-de Bire, A. *Acta Crystallogr.* **1999**, *C55*, 911−913.
(17) (a) *Neutron Scattering from Magnetic Materials*; Tapan, C., Ed.; Elsevier: Boston, MA, 2006. (b) Izyumov, Y. A.; Naish, V. E.; Ozerov, R. P. *Neutron Diffaction of Magnetic Materials*; Consultants Bureau: New York, 1991.
(18) (a) Sibille, R.; Lhotel, E.; Mazet, T.; Malaman, B.; Ritter, C.; Ban, V.; François, M. *Phys. Rev. B* **2014**, *89*, No. 104413. (b) Cañadillas-Delgado, L.; Fabelo, O.; Rodríguez-Velamazán, J. A.; Lemee-Cailleau, M. H.; Mason, S. A.; Pardo, E.; Lloret, F.; Zhao, J. P.; Bu, X. H.; Simonet, V.; Colin, C. V.; Rodríguez-Carvajal, J. *J. Am. Chem. Soc.* **2012**, *134*, 19772−19781. (c) Baker, M. L.; Mutka, H. *Eur. Phys. J.: Spec. Top.* **2012**, *213*, 53−68. (d) Fabelo, O.; Cañadillas-Delgado, L.; Puente Orench, I.; Rodríguez-Velamazán, J. A.; Campo, J.; Rodríguez-Carvajal, J. *Inorg. Chem.* **2011**, *50*, 7129−7135. (e) Mesbah, A.; Sibille, R.; Mazet, T.; Malaman, B.; Lebegue, S.; Francois, M. *J. Mater. Chem.* **2010**, *20*, 9386−9391. (f) Pellaux, R.; Schmalle, S. W.; Huber, R.; Fischer, P.; Hauss, T.; Ouladdiaf, B.; Decurtins, S. *Inorg. Chem.* **1997**, *36*, 2301−2308.
(19) Thuéry, P. *CrystEngComm* **2014**, *16*, 1724−1734.
(20) Carlin, R. L. *Magnetochemistry*; Springer-Verlag: Berlin, 1986.
(21) Otwinowski, Z.; Minor, W. *Processing of X-ray Diffraction Data Collected in Oscillation Mode*, Methods in Enzymology, Vol. *276*: Macromolecular Crystallography, part A; Carter, C. W., Jr., Sweet, R. M., Eds.; Academic Press: New York, 1997; pp 307−326.
(22) Sheldrick, G. M. *Acta Crystallogr. A* **2008**, *64*, 112−122.
(23) Spek, A. L. *J. Appl. Crystallogr.* **2003**, *36*, 7−13.
(24) Brandeburg, K.; Putz, H. *DIAMOND 2.1d*, Crystal Impact GbR: Bonn, Germany, 2000.
(25) Rodríguez-Carvajal, J. *Phys. Rev. B* **1992**, *192*, 55−69 The programs of the FullProf Suite and their documentation can be obtained from Web at http//:www.ill.eu/sites/fullprof/.
(26) The topological analysis has been done by using the TOPOS 4.0 program: Blatov, V. A. *IUCr CompComm. Newsl.* **2006**, *7*, 4−38.
(27) Stiefel, E. I.; Brown, G. F. *Inorg. Chem.* **1972**, *11*, 434−436.
(28) Margulis, T. N. *J. Am. Chem. Soc.* **1971**, *93*, 2193−2195.
(29) Lines, M. E. *J. Chem. Phys.* **1971**, *55*, 2977−2984.
(30) (a) Zhang, X. H.; Hao, Z. M.; Zhang, X. M. *Chem.—Eur. J.* **2011**, *17*, 5588−5594. (b) Lloret, F.; Ruiz, R.; Julve, M.; Faus, J.; Journaux, Y.; Castro, I.; Verdaguer, M. *Chem. Mater.* **1992**, *4*, 1150−1153.
(31) Rodríguez-Carvajal, J. ILL-August 2007 k-Search program.
(32) Bertaut, E. F. *Acta Crystallogr. A* **1968**, *24*, 217−231.
(33) Rodríguez-Carvajal, J. ILL-August 2007 BasIreps program.
(34) Litvin, D. B. *Acta Crystallogr.* **2001**, *A57*, 729−730.


dx.doi.org/10.1021/ic500443t | *Inorg. Chem.* XXXX, XXX, XXX−XXX